Cosmic tides in view of halos

Tian-Xiang Mao,[1,2] Hong-Ming Zhu,[1,2] Ue-Li Pen,[3,4,5,6] Yu Yu,[7] Xuelei Chen,[1,2,8] and Jie Wang[1]

[1]*Key Laboratory for Computational Astrophysics, National Astronomical Observatories, Chinese Academy of Sciences, 20A Datun Road, Beijing 100012, China*
[2]*University of Chinese Academy of Sciences, Beijing 100049, China*
[3]*Canadian Institute for Theoretical Astrophysics, University of Toronto, 60 St. George Street, Toronto, Ontario M5S 3H8, Canada*
[4]*Dunlap Institute for Astronomy and Astrophysics, University of Toronto, 50 St. George Street, Toronto, Ontario M5S 3H8, Canada*
[5]*Canadian Institute for Advanced Research, CIFAR Program in Gravitation and Cosmology, Toronto, Ontario M5G 1Z8, Canada*
[6]*Perimeter Institute for Theoretical Physics, 31 Caroline Street North, Waterloo, Ontario, N2L 2Y5, Canada*
[7]*Key laboratory for research in galaxies and cosmology, Shanghai Astronomical Observatory, Chinese Academy of Sciences, 80 Nandan Road, Shanghai 200030, China*
[8]*Center of High Energy Physics, Peking University, Beijing 100871, China*

(Dated: October 14, 2016)

PACS numbers:

I. INTRODUCTION

The large-scale structure contains a wealth of information about our Universe. By measuring large-scale structure we can attempt to find the answers to such fundamental questions as what the initial conditions of the Universe are and what its future will be. There have been a lot of efforts in measuring the large-scale structure of our Universe (e.g. SDSS, something about DR12). However, the mode coupling because of nonlinear evolution (here add citation) and many other observational problems (such as RSD) make it difficult to extract cosmological information. Additionally, because of the limited volume of surveys, uncertainties due to sample variance is also difficult to overcome.

Dark matter halos, which host observable galaxies and galaxy clusters, are the fundamental nonlinear units of cosmic structure. On large scales, dark matter halos can be considered as biased tracers of the underlying dark matter distribution [1]. Not only the local matter distribution but also the large-scale environment can affect the shapes, the abundance, the accretion, the bias, and the power spectrum of halos [2–9]. So the coupling between the large-scale environment and small-scale density fluctuation may be used to extract more information about the large-scale structure, which is helpful to suppress the sample variance of large-scale modes. In recent studies, this effect is used to get the information of very long-wavelength modes outside the survey volume by considering the large-scale environment contribute to the mean density fluctuation in the survey (or "separate universe") [10–15]. Nevertheless, the isotropic distortions on small scales may derived from not only the large-scale environment but also some other processes. In our previous stydies [16, 17], the long-wavelength tidal field is reconstructed by quantifying the local anisotropy of small-scale density statistics and even a better result obtained by a developed 3-D method [**?**].

In this paper, we investigate the cosmic tidal reconstruction in view of halos. Different with dark matter density field, reconstruction with halos field has many advantages. In the dark matter case, we need to take a logarithmic transform or map the density fluctuations into a Gaussian distribution to Gaussianize the smoothed density field or suppress the high weights of the high density regions because of quadratic estimator [16**?** , 17]. However, for halo counts, there is not such problems. Without Gaussianization, we can quantify the bias of reconstruction easier and get a simpler and clearer physical picture, which we will discuss in III. Additionally, since most observed tracers of large-scale structure, such as galaxies, reside in halos, the statistics of halos determine galaxies on large scale. So the study of halos reconstruction is helpful for studying the reconstruction with galaxy surveys, which we will study in the future.

On large scales, the relation between halo and dark matter can be modeled by a bias factor $b(k)$ and numerous studies have been made about it [4, 18–25]. As a biased tracer of dark matter, halos with different mass trace dark matter in different degrees. So can we get a better result in reconstruction by dealing different halos with different ways is an interesting thing. In addition, the shot noise, which due to the discrete sampling of halos, always assumed to the inverse of the number density $1/\bar{n}$, is another problem that should be solved. Here, we apply a wiener filter to suppress the shot noise, which we will introduce later.

(*)This paper is organized as follows. In Section II, we review the reconstruction technique. In Section III, we study the performance of reconstruction in halo density fields from N-body simulations. In Section **??**, we study how much improvement can get from bias weighted halo fields.

II. REVIEW OF TIDAL RECONSTRUCTION

The basic idea of cosmic tidal reconstruction is introduced originally in Ref. [16] and detailed description can be found in Ref. [17]. In this section we will briefly review it.

Not only the small-scale density fluctuation but also the long-wavelength tidal field influence the evolution of local small-scale density field. The local anisotropic distortion, which derived from the long-wavelength traceless tidal field $t_{ij} = \Phi_{L,ij} - \delta_{ij}\nabla^2\Phi_L/3$, where Φ_L is the long-wavelength gravitational potential, can be used to reconstruct the large-scale density field. If we just assume the leading-order coupling between the long-wavelength tidal field and small-scale density field, the tidal distortion of the local small-scale power spectra can be written as

$$P(\boldsymbol{k},\tau)|_{t_{ij}} = P_{1s}(k,\tau) + \hat{k}^i\hat{k}^j t_{ij}^{(0)} P_{1s}(k,\tau) f(k,\tau), \quad (1)$$

where $\hat{k}$ is the unit vector in the direction of $\boldsymbol{k}$, P_{1s} is the isotropic linear power spectrum and $f(k,\tau)$ are used to describe the coupling of the long-wavelength tidal field and small-scale density field. Here, the superscript (0) and τ are denote the "initial" time and conformal time, respectively.
Here, the filter $f(\boldsymbol{k},\tau)$ is defined as

$$f(k,\tau) = 2\alpha - \beta\frac{d\ln P_{1s}(k,\tau)}{d\ln k}, \quad (2)$$

where

$$\begin{aligned}\alpha(\tau) &= -D_{\sigma 1}(\tau) + F(\tau),\\ \beta(\tau) &= F(\tau),\end{aligned} \quad (3)$$

with

$$D_{\sigma 1}(\tau) = \int_0^\tau d\tau' \frac{H(\tau)D(\tau') - H(\tau')D(\tau)}{\dot{H}(\tau')D(\tau') - H(\tau')\dot{D}(\tau')}\frac{T(\tau')D(\tau')}{D(\tau)}, \quad (4)$$

$$F(\tau) = \int_0^\tau d\tau'' a(\tau'')T(\tau'')\int_{\tau''}^\tau d\tau'/a(\tau'). \quad (5)$$

Here, $D(\tau)$ is the linear growth factor, $T(\tau) = D(\tau)/a(\tau)$ is the linear transfer function and $H(\tau) = d\ln a/d\tau$ is the comoving Hubble parameter.

The tensor $\Phi_{L,ij}$ can be written as

$$\Phi_{L,ij} = \delta_{ij}\kappa + t_{ij}, \quad (6)$$

where the convergence field $\kappa = \nabla^2\Phi_L/3$.
The traceless tidal tensor t_{ij} can be decomposed as in weak lensing:

$$t_{ij} = \begin{pmatrix}\gamma_1 - \gamma_z & \gamma_2 & \gamma_x\\ \gamma_2 & -\gamma_1 - \gamma_z & \gamma_y\\ \gamma_x & \gamma_y & 2\gamma_z\end{pmatrix}, \quad (7)$$

where $\gamma_1 = (\Phi_{L,11} - \Phi_{L,22})/2$, $\gamma_2 = \Phi_{L,12}$, $\gamma_x = \Phi_{L,13}$, $\gamma_y = \Phi_{L,23}$, $\gamma_z = (2\Phi_{L,23} - \Phi_{L,11} - \Phi_{L,22})/6$.

And under the Gaussian assumption and in the long-wavelength limit, the optimal tidal shear estimators can be given as (more details can found in Ref. [17])

$$\begin{aligned}\hat{\gamma}_1 &= \left[\delta^{w_1}(x)\delta^{w_1}(x) - \delta^{w_2}(x)\delta^{w_2}(x)\right],\\ \hat{\gamma}_2 &= [2\delta^{w_1}(x)\delta^{w_2}(x)],\\ \hat{\gamma}_x &= [2\delta^{w_1}(x)\delta^{w_3}(x)],\\ \hat{\gamma}_y &= [2\delta^{w_2}(x)\delta^{w_3}(x)],\\ \hat{\gamma}_z &= [2\delta^{w_3}(x)\delta^{w_3}(x) - \delta^{w_1}(x)\delta^{w_1}(x) - \delta^{w_2}(x)\delta^{w_2}(x)]/3,\end{aligned} \quad (8)$$

where $\delta^{w_i}(x)$ are filtered density fields

$$\delta^{w_i}(\boldsymbol{k}) = \delta(\boldsymbol{k})w_i(\boldsymbol{k}). \quad (9)$$

and $i = 1, 2, 3$ indicates $\hat{x}$, $\hat{y}$ and $\hat{z}$ directions. In the dark matter case, a Gaussianization method is needed because the Gaussian assumption. However, for halo reconstruction, the Gaussianization is not performed for some reasons, which we will discuss in Sec. III. In Fourier space, $w_i(\boldsymbol{k})$ is given by

$$w_i(\boldsymbol{k}) = \mathrm{i}\hat{k}_i\left[\frac{P(k)f(k)}{QP_{tot}^2(k)}\right]^{1/2}, \quad (10)$$

with

$$Q = \int\frac{2k^2dk}{15\pi^2}\frac{P^2(k)}{P_{tot}^2(k)}f^2(k). \quad (11)$$

Here, $f(k)$ is from Eq. (2) and more details will also discussed in Sec. III.

Then, the convergence term κ can be estimated from shear terms γ_i

$$\begin{aligned}\kappa(\boldsymbol{k}) = \frac{1}{k^2}[&(k_1^2 - k_2^2)\gamma_1(\boldsymbol{k}) + 2k_1k_2\gamma_2(\boldsymbol{k}) + 2k_1k_3\gamma_x(\boldsymbol{k})\\ &+ 2k_2k_3\gamma_y(\boldsymbol{k}) + (2k_3^2 - k_1^2 - k_2^2)\gamma_z(\boldsymbol{k})],\end{aligned} \quad (12)$$

and the large-scale density field can be given by the convergence field because of the Poisson equation.
To correct the bias and reduce the noise in reconstructed field, we write the reconstructed clean field $\hat{\kappa}$ as

$$\hat{\kappa}(k_\perp, k_\parallel) = \frac{\kappa(k_\perp, k_\parallel)}{b(k_\perp, k_\parallel)}W(k_\perp, k_\parallel), \quad (13)$$

where bias factor

$$b(k_\perp, k_\parallel) = \frac{P_{\kappa\delta}(k_\perp, k_\parallel)}{P_{\delta\delta}(k_\perp, k_\parallel)} \quad (14)$$

and Wiener filter

$$W(k_\perp, k_\parallel) = \frac{P_{\delta\delta}(k_\perp, k_\parallel)}{P_{\kappa\kappa}(k_\perp, k_\parallel)/b^2(k_\perp, k_\parallel)}. \quad (15)$$

Here, the noise power spectrum is

$$P_n(k_\perp, k_\parallel) = P_{\kappa 3\mathrm{D}}(k_\perp, k_\parallel) - b^2(k_\perp, k_\parallel)P_{\delta\delta}(k_\perp, k_\parallel). \quad (16)$$

III. PERFORMANCE OF RECONSTRUCTION

In this section we perform reconstruction in simulated halos fields, following almost the same process in previous papers. To better understand the discrepancy between reconstruction in dark matter and halos, we discuss the bias and noise of halos, which tell us how to decrease the halos noise in reconstruction. And then, we also use the cross-correlation coefficient to quantify the result of reconstruction and discuss the bias and noise of it.

A. Simulation

(*)We run N-body simulations using the CUBEP^{3}M code with 2048^3 dark matter particles in a box of side length $L = 1.2$ Gpc/h. We have adopted the following set of cosmological parameter values: $\Omega_b = 0.049$, $\Omega_c = 0.259$, $h = 0.678$, $A_s = 2.139 \times 10^{-9}$ and $n_s = 0.968$. Ten runs with independent initial conditions were performed to provide better statistics. In the following calculations we use outputs at $z = 0$.

B. Properties of halos fields

In this subsection, we choose three different number-density (0.0048 h^3Mpc^{-3}, 0.0024 h^3Mpc^{-3} and 0.0012 h^3Mpc^{-3}) halos fields to show the properties of halos fields. here, describe how to get these halos fields with different number density and the mass of each halos field. And it may be added in subsection of Simulation

In Fig. 1, we show the bias factor of simulated halos fields in three different number densities. Here we define the halos bias factor as $b_h(k) = P_{\delta h}(k)/P_{\delta\delta}(k)$, which without the shot noise $1/\bar{n}$. Here, the $P_{\delta\delta}(k)$ and $P_{\delta h}$ are the auto-correlation power spectrum of dark matter and the halo-matter cross-correlation power spectrum. The dashed, the dash-dotted and the dotted lines show the bias of halos fields with number density 0.0012 h^3Mpc^{-3}, 0.0024 h^3Mpc^{-3} and 0.0048 h^3Mpc^{-3}, respectively. The solid line with corresponding color is the linear bias obtained by averaging the first 6 k-bins ($k < 0.04$ h/Mpc) of $b_h(k)$. On small scales, the bias is no longer a scale-independent factor. In this paper, every point is averaged all ten simulations and the error is given by the bootstrap.

The shot noise and stochasticity of halos are always an important and complicated topic in relevant studies cite here. A batter understanding about the shot noise and stochasticity is helpful to decrease its influence in our reconstruction (in this paper, a wiener filter is applied to suppress the noise in halos fields, which we discuss this further below). The shot noise, assumed roughly to $1/\bar{n}$ here, can be subtract from the halos auto-cross power spectrum. (Although some papers suggest the shot-noise subtraction is not safely.. may cite here?) And note that the matter power spectrum dose not require shot noise subtraction because of the large number of dark matter

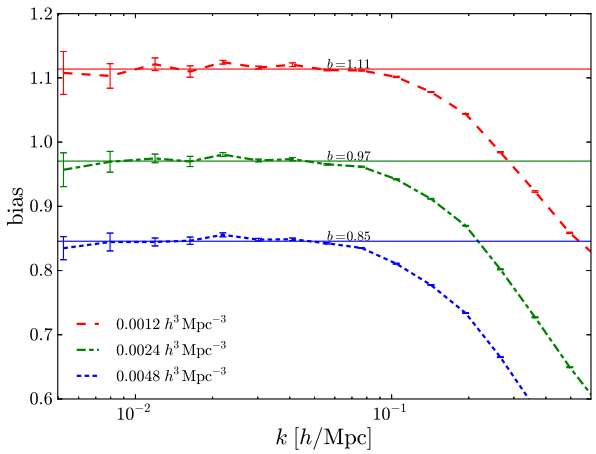

FIG. 1: Halo biases of different number-density halos fields. The dashed, the dash-dotted and the dotted line shows the bias of halos fields with different number density. And linear biases (horizontal solid lines) are obtained by averaging the first 6 k-bins ($k < 0.04$ h/Mpc) for each line.

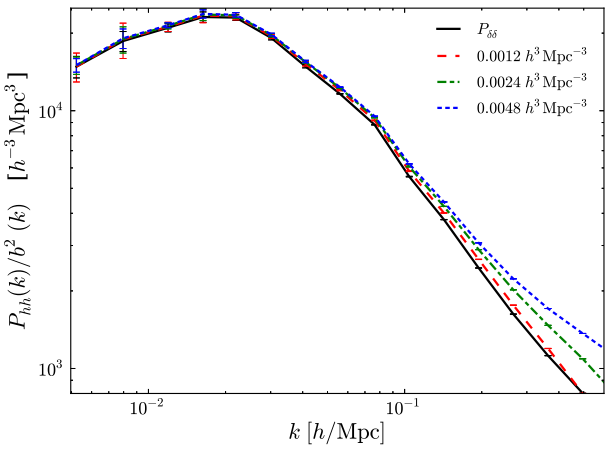

FIG. 2: Top panel: the auto-power spectrum of halo fields. The solid lines are the power spectrum of halo fields with number density of 0.0048 h^3Mpc^{-3}, 0.0036 h^3Mpc^{-3}, 0.0024 h^3Mpc^{-3} and 0.0012 h^3Mpc^{-3}, respectively. The horizontal dot dash lines are corresponding shot noise $1/\bar{n}$ for every halo fields. Here $\bar{n}$ is the number density. The black dashed line is the power spectrum of dark matter field. Bottom panel: same as the top panel, but the colored solid lines are the matter-halo cross power spectrum.

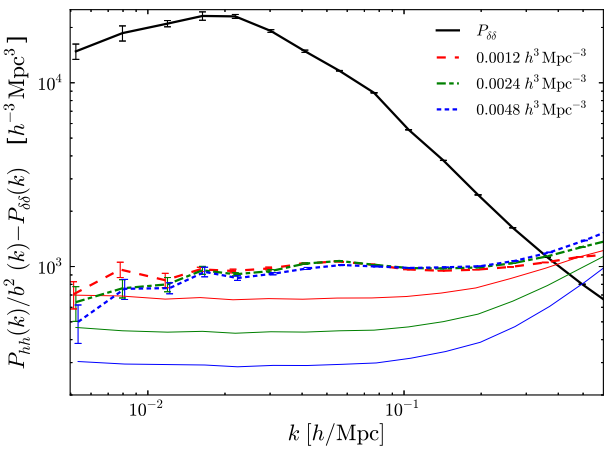

FIG. 3: Top panel: the auto-power spectrum of halo fields. The solid lines are the power spectrum of halo fields with number density of 0.0048 h^3Mpc^{-3}, 0.0036 h^3Mpc^{-3}, 0.0024 h^3Mpc^{-3} and 0.0012 h^3Mpc^{-3}, respectively. The horizontal dot dash lines are corresponding shot noise $1/\bar{n}$ for every halo fields. Here $\bar{n}$ is the number density. The black dashed line is the power spectrum of dark matter field. Bottom panel: same as the top panel, but the colored solid lines are the matter-halo cross power spectrum.

particles. In Fig. 2, we plot the power spectra of three different number-density halos fields. To compare these power spectra with dark matter power spectra, halos shot-noise subtracted auto-correlation power spectra is divided by square of the bias factor $P_{hh}(k)/b^2(k)$ (here, the bias we use is the scale-dependent bias and see Fig. 1). Here, the black solid line is the matter power spectrum and coloured lines indicate the halos auto-correlation power spectra of different number density as in Fig. 1. We find, on large scales, different power spectra are almost have a same value. Which suggest even with only shot-noise subtraction, the halos power spectra can trace the dark matter power well (less relative error) on large scales in choosed number density and halo mass. However, on small scale, the halos power spectra are always above the dark matter power even applied the shot-noise subtraction, and higher number density with larger difference. So if we want to quantify the noise of halos fields, consider the shot noise only is not enough, especially on small scale.

Understanding everything about the shot noise and the stochasticity is too complex and difficult, but it worth the effort. However, we do not need to do it in our reconstruction. Here, we define the noise power of halos field

$$P_n(k) = P_{hh}(k) - b_h^2(k)P_{\delta\delta}(k), \tag{17}$$

in which both the shot noise and the stochasticity have contribution. By this equation, we can calculate the noise of halos from simulations. In Fig. 3, we plot the $P_n(k)/b_h^2(k)$ to compare with the dark matter power spectrum (the black solid line). Identical to 2, we use the dashed, the dash-dotted and the dotted line show the noise power of different number density. Three thin coloured solid lines indicate the shot noise of corresponding number density, which have been divided by $b_h^2(k)$ too. In this way, we can compare the shot noise $1/\bar{n}$, the noise of halos $P_n(k)$ and the power of dark matter $P_{\delta\delta}(k)$ directly. On the linear scales ($k < 0.1$ h/Mpc), all the noise lines is over the corresponding shot noise line, which is because of stochasticity. And comparing to the shot noise, the noise power P_n is almost have the same order, which meaning the noise is dominated by stochasticity on large scale in choosed number density and halo mass. In nonlinear region, the nonlinear evolution involve much complex effects, we do not discuss it here. The correlation coefficient of halos and dark matter, which defined as $r_{\rm h} = P_{\delta h}/\sqrt{P_{\delta\delta}P_{hh}}$, is always used to quantify the relation between the distribution of halo and matter. From Eq. 17 and the definition of $b_h(k)$ we can prove $\frac{P_n/b_h^2}{P_{\delta\delta}} = \frac{1}{r_{\rm h}^2} - 1$, so we do not show the correlation coefficient here.

By these discussion about the bias, the power and the noise of halos fields, we hope to find the differences between the reconstruction in halos and dark matter, which we discuss in subsection III C.

C. Performance of reconstruction

The performance of reconstruction in halos mainly following the previous works [16, 17]. However, there are some changes because of the differences between the dark matter and halo fields. Note that because we are using the halos fields to trace dark matter distribution, the $\delta(x)$ used here is the halos density field (explain how to get halos density field in Simulation or it should be another name?) which have deconvolved bias b_h. The algorithm of the reconstruction in halos is as follows.
(i). Applying a Gaussian smoothing kernel to $\delta(x)$:

$$\bar{\delta}(\mathbf{x}) = \int d^3x' \mathbf{S}(\mathbf{x}-\mathbf{x}')\delta(\mathbf{x}'), \tag{18}$$

where $\mathbf{S}(r) = \mathrm{e}^{-r^2/2R^2}$ and R is the smoothing scale. Here, we calculated a lots of different smoothing scales and find we can obtain the optimal reconstruction result with the smoothing scale $R = 1.0$ Mpc/h. So we select $R = 1.0$ Mpc/h as the smoothing scale in this paper. By this step, we get a smoothed field $\bar{\delta}_h(x)$ which is considered as the cosmic density field and have been suppressed the vary small-scale fluctuations.
discuss why different number-density halos reconstruction with the same smoothing scale in Sec. Discussion.
(ii). Convolving the smoothed density field $\bar{\delta}_h(x)$ with a wiener filter (about the Wiener and δ^{w_i} should be discussed in Sec. Discussion: why we separate the Wiener

from filter w_i.)

$$W_h(k) = \frac{P_{hh}(k) - P_n(k)}{P_{hh}(k)} = \frac{b_h^2(k) P_{\delta\delta}(k)}{P_{hh}(k)}, \qquad (19)$$

where $P_{hh}(k)$ is the without shot-noise subtracted halos power spectrum, $P_{\delta\delta}(k)$ the dark matter power spectrum, $b_h(k)$ the bias factor of halos and $P_n(k)$ the noise power from Eq. 17.

The Wiener filter is help to suppress the noise of halos fields if we know the signal and noise accurately. However, in real data, there is no approach to distinguish the signal and noise exactly, but we can in simulation. So the Wiener filter should be calculated in simulations. The halos bias factor $b_h(k)$ used here is a scale-dependent bias. However, a linear bias factor is usually believed more credible and can be obtained from observation. In the Sec. IV here cite the figure , we will show that it is no influence on the reconstruction whether the scale-dependent (the curved lines in Fig. 1) or the scale-independent (the horizontal solid lines in Fig. 1) bias is used here.

After applying Eq. (19), we suppress the noise in halo field (both the shot noise and stochasticity) and obtain a smoothed and filtered halo density field $\tilde{\delta}(x)$ to reconstruction.

(iii).* Then, we convolve the smoothed and filtered density field $\tilde{\delta}(x)$ with w_i (from Eq. 10) and calculate γ_1, γ_2, γ_x, γ_y and γ_z by Eqs. (8)(10)(11). And by Eq. (12) we obtain 3D convergence field $\kappa(\boldsymbol{k})$.

(iv).* By Eq. (13), we correct the bias and suppress the noise of the estimated convergence field $\hat{\kappa}$. Here, $b(k_\perp, k_\parallel)$ and $W(k_\perp, k_\parallel)$ are calculated by averaging in all ten simulations. need discuss how to get reconstructed large-scale δ_L from $\hat{\kappa}$?

The tidal shear estimator is an optimal estimator under the Gaussian assumption, which have discussed in Ref. [17]. However, we do not apply a Gaussianization method here. This is because of the following points. Firstly, different from the dark matter density field, halos counts have not such high fluctuations on small scale. So it is not necessary to Gaussianize to suppress the high weights of the high density regions because of quadratic estimator. Secondly, for halos-counts fields, there are many grids without halos, which makes the Gaussianization method lead into some other problems.

D. Result

In this subsection, we introduce the result of reconstruction by showing the power spectra, the correlation coefficient, the bias and the noise of reconstructed density field κ.

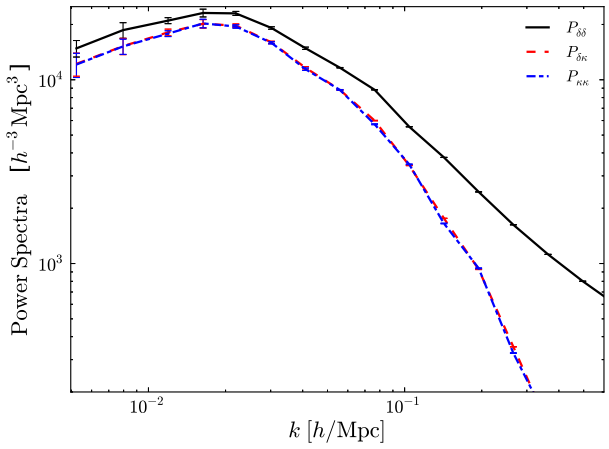

FIG. 4: Auto-power spectrum of dark matter, halo and reconstructed κ fields and cross-power spectrum of matter-halo and matter-kappa, respectively. Here the number density of halo fields is 0.0024 $h^3\mathrm{Mpc}^{-3}$ and the smoothing scale is $R = 1.0$ Mpc/h.

Here, the correlation coefficient of reconstructed density field κ and dark matter density field defined as

$$r_\mathrm{r}(k) = \frac{P_{\kappa\delta}(k)}{\sqrt{P_{\delta\delta}(k) P_{\kappa\kappa}(k)}}, \qquad (20)$$

the bias factor

$$b_\mathrm{r}(k) = \frac{P_{\kappa\delta}(k)}{P_{\delta\delta}(k)}, \qquad (21)$$

and the noise

$$\tilde{P}_n(k) = P_{\kappa\kappa}(k) - b_\mathrm{r}^2(k) P_{\delta\delta}(k). \qquad (22)$$

In Fig. 4, we show the auto-correlation power spectra of reconstructed kappa and dark matter density field and the kappa-matter cross power spectrum is also plotted. Here, we reconstruct with halos number density as 0.0024 $h^3\mathrm{Mpc}^{-3}$ and the subscript κ is the reconstructed large-scale density field $\hat{\kappa}$ which has corrected bias and convolved Wiener filter by Eq. 13, the δ indicates the original dark matter density field. The high errors on the first two k bins is because of the sample variance. And we find on large scales ($k < 0.1h$/Mpc), $P_{\delta\kappa}$ and $P_{\kappa\kappa}$ almost have the same shape with $P_{\delta\delta}$. Then the power of $P_{\delta\kappa}$ and $P_{\kappa\kappa}$ drop quickly. The almost coincidence of $P_{\delta\kappa}$ and $P_{\kappa\kappa}$ here is because of the Wiener filter in Eq. 13.

In Fig. 5, we show the correlation coefficients (see Eq. (20)) of reconstructed density field κ and dark matter density field δ . Here we choose the number density of halos fields as 0.0012 $h^3\mathrm{Mpc}^{-3}$, 0.0024 $h^3\mathrm{Mpc}^{-3}$ and 0.0048 $h^3\mathrm{Mpc}^{-3}$ (here, the Fig. 4 is corresponding to the green dash-dotted line) and apply a smoothing kernel with $R = 1.0$ Mpc/h (Eq. (18)). We also plot the

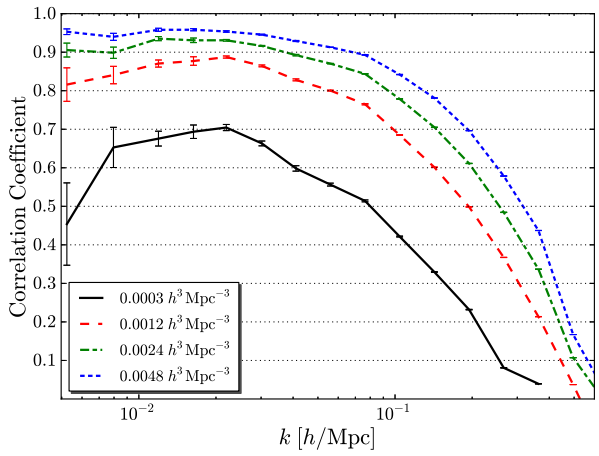

FIG. 5: Correlation coefficient of reconstructed convergence density field κ and dark matter density field δ (Eq. (20)). Here we choose the number density of halos fields as 0.0012 h^3Mpc^{-3}, 0.0024 h^3Mpc^{-3} and 0.0048 h^3Mpc^{-3} and apply a smoothing kernel with $R = 1.0$ Mpc/h (Eq. (18)). We also plot the correlation coefficient of the reconstructed field from halo fields with number density of 0.0003 h^3Mpc^{-3}, which is the average number density of BOSS.

correlation coefficient of the reconstruction from halos fields with number density of 0.0003 h^3Mpc^{-3}, which is the average number density of BOSScite here. For the highest number-density (0.0048 h^3Mpc^{-3}) reconstruction, the correlation coefficient $r_{\rm r}$ is larger than 0.9 in almost all $k < 0.1$ h/Mpc. What's more, even for the 0.0003 h^3Mpc^{-3} number-density halos, the reconstruction can also obtain a result of $r_{\rm r} > 0.5$ in nearly all $k < 0.1$ h/Mpc. Obviously, lower number-density halos means less information about dark matter and lead to the loss of correlation coefficient. And the errors also increase with the dropping of halos number density. should mention the number density of MGS here?

The cosmic tidal reconstruction recover the information lies at small scales and the long wavelength modes contribute little [17, 26]. So if we apply a high-pass filter to remove the large-scale modes (here, we remove the modes where $k < 0.1$ h/Mpc) of halos fields in Fourier space, the reconstruction of high-pass filtered halos fields should only lose little. In Fig. 6, on the top panel: we plot the with and without high-pass filtered halos power spectra $P_{hh}^{k>0.1}$ and P_{hh}, respectively. And the power spectrum of reconstructed density fields from high-pass filtered halos fields $P_{\kappa\kappa}^{k>0.1}$ is shown in green dotted line. Here, the $P_{\delta\delta}$ (the black thin solid line) is the power of original dark matter density fields. All the power spectrum is divided by the square of bias factor between dark matter to compare together. We see only with the small-scale density fluctuation (the red thick solid line) can we reconstruct the large scale density field (the green dotted line). Here, the first point of $P_{hh}^{k>0.1}$

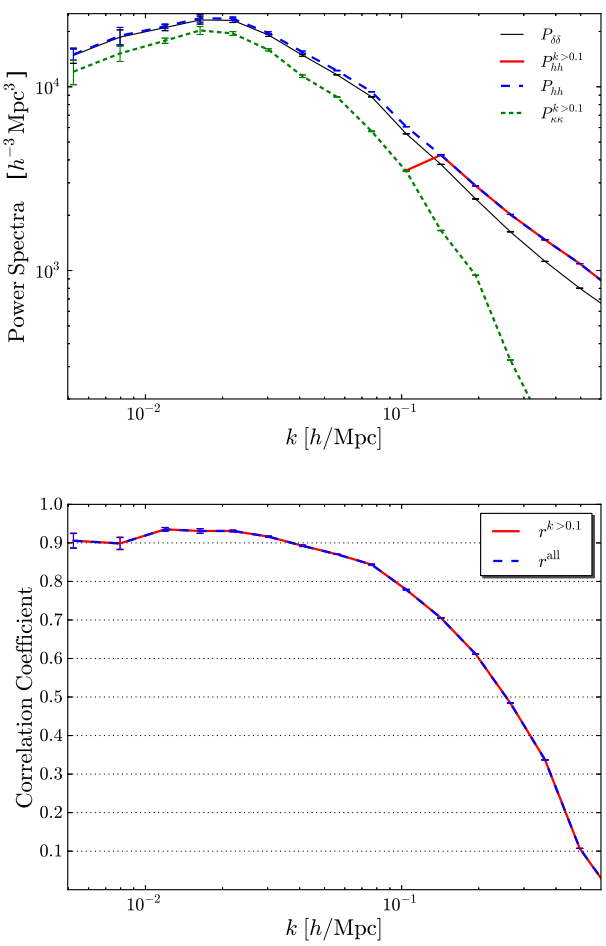

FIG. 6: For high-pass filtered test.

is because this k-bin includes modes both which are removed by high-pass filter and which are not removed. On the bottom panel: the $r^{\rm all}$ and $r^{k>0.1}$ indicate the correlation coefficients of dark matter and reconstructed density field by halos and high-pass filtered halos fields, respectively. We find even reconstruct without the large-scale ($k < 0.1$ h/Mpc) modes of halos can also obtain a result as good as we do with all k modes. It matches the discussion previous.

E. bias and noise

As in III B, we analyse the result of reconstruction by the bias factor (defined in Eq. 21) and the noise (defined in Eq. 22) of reconstructed density fields.

Fortunately, in halos view, it is not necessary to take the effect of Gaussianization into account and we can try to quantify the bias because of the estimator. When we

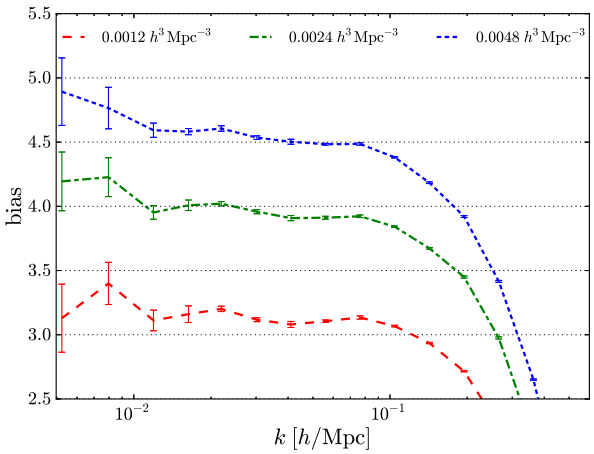

FIG. 7: Bias factor $b(k)$ of reconstructed κ field from different number density halo fields (Eq. (14)). Here we correct the bias by Eq. (24) and get the constant bias of reconstruction as 4.66, 4.06 and 3.19 for reconstructed κ fields from 0.0048 h^3Mpc^{-3}, 0.0024 h^3Mpc^{-3} and 0.0012 h^3Mpc^{-3}, respectively. Here, the constant bias is obtained by averaging the bias of the first 6 k-bins.

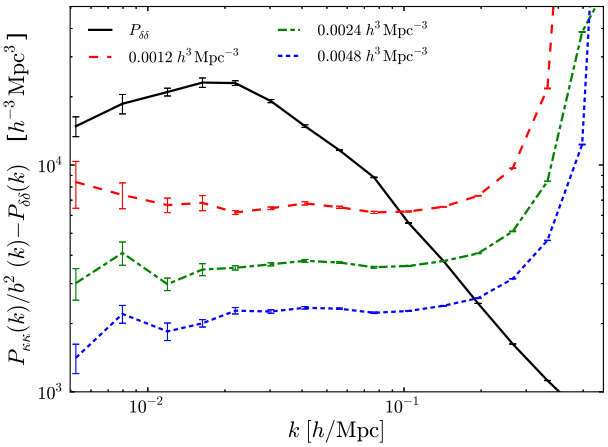

FIG. 8: The noise spectrum of reconstruction. Here we define the noise spectrum as $P_n(k) = P_\kappa(k)/b^2(k) - P_\delta(k)$ and the bias $b(k) = P_{\kappa\delta}(k)/P_{\delta\delta}(k)$ is a k-dependent bias. Four colored solid lines are corresponding different number density of halos fields.

calculate the bias, the Wiener filter and the Gaussian smoothing kernel should be involved in Q factor (in Eq. (11)) and the bias because of halos and dark matter b_h (see Fig. 1) also need to be corrected.

Because of the smoothing kernel we used in Eq. (18) and the Wiener filter in Eq. (19), the Q factor becomes:

$$Q = \int \frac{2k^2 dk}{15\pi^2} W_h^2(k) S^2(k) f^2(k), \tag{23}$$

Here, we solve the Q factor by integrating from the fundamental frequency to the Nyquist frequency in the box of simulations.
Then the Eq. (21) becomes

$$b_{\rm r} = \frac{P_{\kappa\delta}}{P_{\delta\delta}} \frac{1}{b_h^2 Q}. \tag{24}$$

In Fig. 7, we show the isotropic bias factor $b_{\rm r}$ of reconstructed density fields from three different number-density halos fields. The dashed, the dash-dotted and the dotted line is corresponding to the number density of 0.0012 h^3Mpc^{-3}, 0.0024 h^3Mpc^{-3} and 0.0048 h^3Mpc^{-3}, respectively. In these number density, the bias of reconstruction is about $3 \sim 5$ on large scales.

The noise of reconstructed density field is plotted in Fig. 8.

IV. DISCUSSION

[1] N. Kaiser, ApJ **284**, L9 (1984).
[2] S. Chen, H. Wang, H. J. Mo, and J. Shi, ApJ **825**, 49 (2016), 1603.04152.
[3] U. Seljak, J. Cosmology Astropart. Phys. **3**, 004 (2012), 1201.0594.
[4] H. J. Mo and S. D. M. White, MNRAS **282**, 347 (1996), astro-ph/9512127.
[5] J. Shi, H. Wang, and H. J. Mo, ApJ **807**, 37 (2015), 1501.07764.
[6] C.-T. Chiang, C. Wagner, A. G. Sánchez, F. Schmidt, and E. Komatsu, J. Cosmology Astropart. Phys. **9**, 028 (2015), 1504.03322.
[7] Y. Li, W. Hu, and M. Takada, Phys. Rev. D **90**, 103530 (2014), 1408.1081.
[8] C.-T. Chiang, C. Wagner, F. Schmidt, and E. Komatsu, J. Cosmology Astropart. Phys. **5**, 048 (2014), 1403.3411.
[9] M. Takada and W. Hu, Phys. Rev. D **87**, 123504 (2013), 1302.6994.
[10] T. Baldauf, U. Seljak, L. Senatore, and M. Zaldarriaga, J. Cosmology Astropart. Phys. **9**, 007 (2016), 1511.01465.
[11] C.-T. Chiang, Y. Li, W. Hu, and M. LoVerde, ArXiv e-prints (2016), 1609.01701.

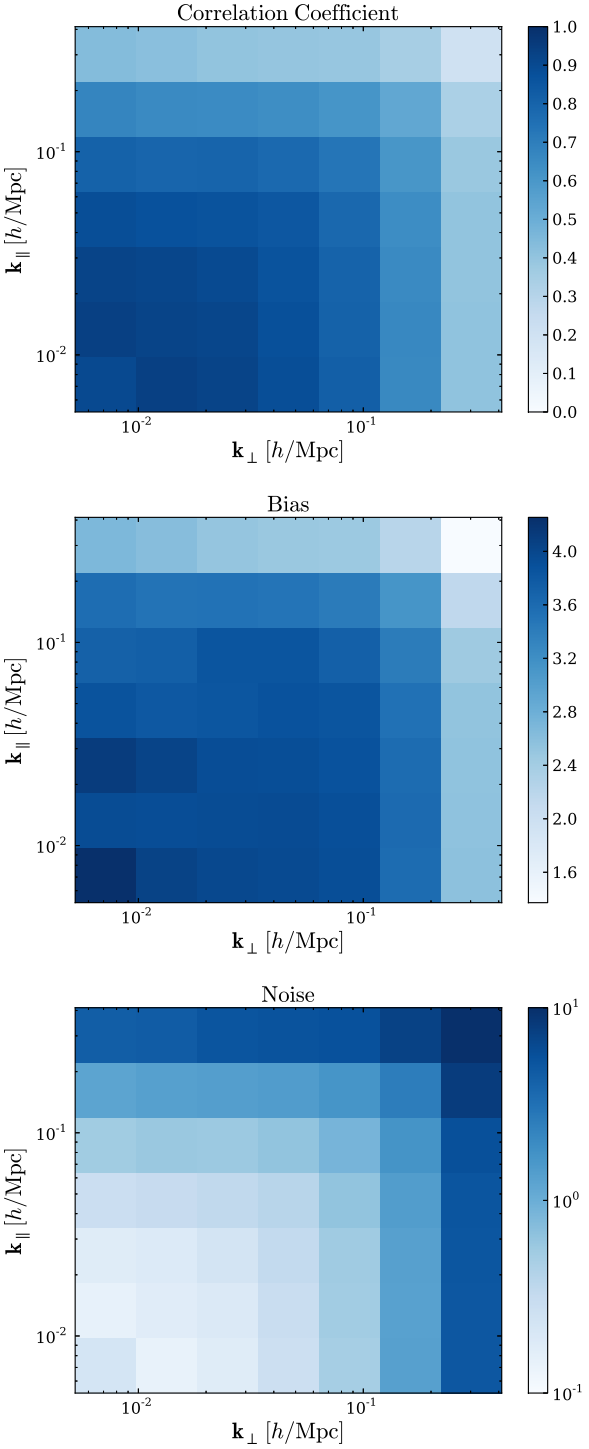

FIG. 9: We plot the 2D correlation coefficient, bias factor and noise of reconstructed κ field from top to bottom, respectively. Here the definition of correlation coefficient and bias factor are same with Fig. 5 and Fig. 7, and the noise in the bottom panel is defined as $(P_\kappa - b^2 P_\delta)/b^2 P_\delta$. All three panels are reconstructed from halo fields with number density of 0.0024 $h^3\mathrm{Mpc}^{-3}$.

[12] Y. Li, W. Hu, and M. Takada, Phys. Rev. D **93**, 063507 (2016), 1511.01454.

[13] T. Lazeyras, C. Wagner, T. Baldauf, and F. Schmidt, J. Cosmology Astropart. Phys. **2**, 018 (2016), 1511.01096.

[14] C. Wagner, F. Schmidt, C.-T. Chiang, and E. Komatsu, J. Cosmology Astropart. Phys. **8**, 042 (2015), 1503.03487.

[15] P. McDonald, ApJ **585**, 34 (2003), astro-ph/0108064.

[16] U.-L. Pen, R. Sheth, J. Harnois-Deraps, X. Chen, and Z. Li, ArXiv e-prints (2012), 1202.5804.

[17] H.-M. Zhu, U.-L. Pen, Y. Yu, X. Er, and X. Chen, Phys. Rev. D **93**, 103504 (2016), 1511.04680.

[18] J. M. Bardeen, J. R. Bond, N. Kaiser, and A. S. Szalay, ApJ **304**, 15 (1986).

[19] R. K. Sheth and G. Tormen, MNRAS **308**, 119 (1999), astro-ph/9901122.

[20] R. K. Sheth, H. J. Mo, and G. Tormen, MNRAS **323**, 1 (2001), astro-ph/9907024.

[21] U. Seljak and M. S. Warren, MNRAS **355**, 129 (2004), astro-ph/0403698.

[22] M. Manera and E. Gaztañaga, MNRAS **415**, 383 (2011), 0912.0446.

[23] J. L. Tinker, B. E. Robertson, A. V. Kravtsov, A. Klypin, M. S. Warren, G. Yepes, and S. Gottlöber, ApJ **724**, 878 (2010), 1001.3162.

[24] T. Baldauf, U. Seljak, L. Senatore, and M. Zaldarriaga, J. Cosmology Astropart. Phys. **10**, 031 (2011), 1106.5507.

[25] T. Sunayama, A. P. Hearin, N. Padmanabhan, and A. Leauthaud, MNRAS **458**, 1510 (2016), 1509.06417.

[26] M. Bucher, C. S. Carvalho, K. Moodley, and M. Remazeilles, Phys. Rev. D **85**, 043016 (2012), 1004.3285.